Dopamine transporters depolarize neurons by a channel mechanism

Lucia Carvelli*, Paul W. McDonald, Randy D. Blakely, and Louis J. DeFelice*

Department of Pharmacology and Center of Neuroscience, Vanderbilt University School of Medicine, Nashville, TN 37232-8548

Edited by Susan G. Amara, University of Pittsburgh School of Medicine, Pittsburgh, PA, and approved September 30, 2004 (received for review May 10, 2004)

Neurotransmitter transporters generate larger currents than expected if one assumes fixed stoichiometry models. It remains controversial, however, whether these depolarizing currents arise from high density and rapid turnover rates of a classical transporter, or whether transporters exhibit bona fide channel behavior. Although heterologously expressed transporters show single-channel behavior and noise analysis in native cells strongly suggests channel behavior, no directly observed single-channel events associated with transporters have been reported thus far in native cells. We describe single-channel events arising directly from the *Caenorhabditis elegans* dopamine transporter (DAT-1) as evidenced by DA-induced channel activity blocked by a high-affinity DAT-1 inhibitor, increased channel activity in neurons that overexpress DAT-1, and loss of channels in *dat-1* knockout neurons. Our data indicate that authentic transporter channels underlie depolarizing whole-cell currents. Thus, DA transporters not only transport DA but also exhibit a channel mode of conduction that directly modulates membrane potential and neuronal function.

Caenorhabditis elegans | dopaminergic neurons | neurotransmitter uptake | single channels and transporters

A unique component of dopamine (DA) neurons is the DA transporter (DAT), responsible for DA uptake in presynaptic terminals (1–3). DAT is expressed on dendrites and axons of mesencephalic DA neurons that innervate the basal ganglia, nucleus accumbens, and frontal cortex, regulating locomotor activity, reward, and attention (4, 5). DAT belongs to a neurotransmitter transporter gene family (SLC6A), whose members translocate neurotransmitters and other solutes into the cell by coupling transport to ion gradients. Transport studies of the Na^+ and Cl^- dependence of DAT indicate that two Na^+ ions and one Cl^- ion are coupled to the movement of each DA^+ molecule that is transported (2, 6–8), indicating that DATs are electrogenic. However, currents mediated by DAT exceed predictions from fixed-coupling stoichiometry, turnover rate, and transporter density (9, 10). Excess currents are also described for the serotonin and norepinephrine transporters, both in reconstituted systems and in native cells (11–15). Patch-clamp experiments reveal that transporter channels have openings and magnitudes comparable to bona fide ion channels (16–20). In addition, data in transfected cells demonstrate channel modes of conduction substrate translocation (21); however, although transporter channels have been inferred from noise analysis in native cells (22) to date, no direct single-channel recordings have been reported in native cells. To better understand the electrophysiological properties of DAT, and to test whether channel modes are intrinsic to DAT or an artifact of heterologous expression, we studied DAT in primary cultures of *Caenorhabditis elegans* DA neurons.

C. elegans is a transparent nematode containing, in the hermaphrodite, eight DA neurons supporting mechanosensory and other modulatory functions (23, 24). *C. elegans* represents a powerful model system for studying neurotransmitter transporter activity because, at the molecular level, all of the fundamental components involved in DA biosynthesis and neurotransmission are conserved, and, at the anatomical and genetic level, the nervous system has been well characterized (25, 26). Furthermore, knockout (ko) animals and other genetic manipulations are relatively straightforward, and primary culture approaches (27) have been developed.

We report, in both native and genetically modified DA neurons, authentic single-channel events associated with the DAT. These unitary events mediate macroscopic currents, which lead to membrane depolarization.

Methods

Plasmid Construction. To establish the NH_2-terminal GFP translational fusion, vector ($P_{dat\text{-}1}$::GFP:DAT-1) was constructed by amplification of the DAT-1 promoter region ($P_{dat\text{-}1}$) from pRN200 (24) by using oligonucleotide primers that added a 5′ *Bam*HI site (RB 1239 5′-CGCCGGATCCAAGCTTCCATGAAATGGAACTTGAATCC-3′) and a 3′ *Pac*I site (RB 1240 5′-CTCCTTAATTAAGGCTAAAAATTGTTGAGATTCGAGTAAACC-3′). This promoter fragment was cloned into pGEMT-easy creating vector pPM001.1 with sequences confirmed by fluorescent dideoxy nucleotide sequencing (Center for Molecular Neuroscience, Vanderbilt University). A point mutation in the promoter was found 407 bp 5′ of the dat-1 ATG. This mutation changed a guanine to an adenine (G to A) and was found in sequences of both N2 genomic preps and the cosmid T23G5, leading us to believe that this is an error in the published *C. elegans* database sequence. The GFP sequences were amplified by PCR by using oligonucleotide primers designed against GFP encoded by pPD95.70 (a gift of A. Fire, Stanford University, Palo Alto, CA), omitting the 5′ nuclear localization signal. We added a *Pac*I site immediately 5′ of the ATG using oligo RB 1247 (5′-CGCCTTAATTAATGAGTAAAGGAGAAGAACTTTTCACTGG-3′) and a 3′ *Asc*I site before the TAG stop codon using RB 1246 (5′-GCTTGGCGCGCCTTTGTATAGTTCATCCATGCCATGTG-3′). The dat-1 cDNA was amplified from plasmid RB454 described previously (28) by using RB 1241 (5′-CGTTGGCGCGCC*G*CAGTTGGTGCCTACAGACG-3′) and RB 1242 (5′-CGGAAGATCTTCATAGCATTATGTCAGAGTGCGG-3′), which added a 3′ *Asc*I site and a 5′ *Bgl*II site, respectively. A guanine residue was added to the beginning of the coding region of dat-1 in the underlined position to place DAT-1 in frame with GFP. Once amplified, both the GFP and dat-1 cDNA were cloned into a pGEMT-easy vector creating pPM001.5 and pPM001.2, respectively. Correct cDNA sequence was verified for both pPM001.5 and pPM001.2 by using T7 and Sp6 oligonucleotides and dye termination sequencing. Once sequences were verified, the dat-1 promoter, GFP, and dat-1 fragments were cloned into a pFA6 vector by using sites added by PCR to create $P_{dat\text{-}1}$::GFP:DAT-1 (pPM005).

This paper was submitted directly (Track II) to the PNAS office.

Abbreviations: ko, knockout; IMP, imipramine; DA, dopamine; DAT, DA transporter; amol, attomole.

*To whom correspondence may be addressed at: Department of Pharmacology, Vanderbilt University, 7130A MRBIII, 465 21st South Avenue, Nashville, TN 37232-8548. E-mail: lucia.carvelli@vanderbilt.edu or lou.defelice@vanderbilt.edu.

Worm Lines. All strains were derived from the WT N2 line and maintained at 20–25°C by using standard methods (29). Transgenic animals containing the transcriptional fusion $P_{dat\text{-}1}$::GFP have been described (24). Transgenic animals containing the NH_2-terminal GFP:DAT-1 fusion protein were created by coinjection of 60 ng/μl $P_{dat\text{-}1}$::GFP:DAT-1, 30 ng/μl plasmid carrier DNA (pBluescript), with 60 ng/μl pRF4 (*rol-6* dominant marker) into the N2 strain. Animals positive for both roll and GFP phenotypes were integrated by using an ultraviolet/trimethylpsoralen protocol (30) and then out-crossed four times to WT. The *dat-1*(*ok157*) strain (24) was a gift of J. Duerr and J. Rand (Oklahoma Medical Research Foundation, Oklahoma City).

***C. elegans* Cell Culture and Heterologous Expression of DAT-1.** Embryonic cells were prepared as described previously (27). We plated 25×10^4 and 10^6 cells per well for electrophysiology and uptake experiments, respectively. SV40 T-antigen transformed HEK-293 cells (tsA-201 cells, generously donated by A. George, Vanderbilt University) were maintained in DMEM high-glucose medium (GIBCO) supplemented with 10% FBS, 2 mM L-glutamine, 100 units/ml penicillin, and 100 mg/ml streptomycin. tsA-201 cells (5×10^4) plated in 24-well plates were transfected with 0.4 μg of DAT-1 or pcDNA3 empty vector cDNA by using FuGENE 6 (Roche). In patch-clamp experiments, 0.4 μg of LRSZ-GFP cDNA was cotransfected with DAT-1 or empty vector plasmids to provide for GFP-based identification of transfected cells. The percentage (typically 70%) of cells GFP-positive was used as the number of cells by which uptake and binding experiments were normalized.

Electrophysiological Recordings and Data Analysis. Whole-cell recordings were performed with an Axopatch 200A amplifier (Axon Instruments, Foster City, CA) by using standard patch-clamp techniques. The sampling frequency was 2.5–5 kHz with a low-pass Bessel filter at 2 or 1 kHz. Currents were digitized with Digidata 1320, collected with pClamp8.3, and analyzed by using AXOGRAPH and ORIGIN 7.0 software (all from Axon Instruments). Pipette resistances for tsA-201 cells were 2–4 MΩ when filled with 120 mM KCl, 10 mM NaCl, 0.1 mM $CaCl_2$, 2 mM $MgCl_2$, 1.1 mM EGTA, 10 mM Hepes, 10 mM dextrose, and 1 mM ATP (magnesium salt) (pH 7.35). The external solution for tsA-201 cells contained 130 mM NaCl or NMDG salt in Na-free buffer, 10 mM Hepes, 1.5 mM $CaCl_2$, 0.5 mM $MgCl_2$, 1.3 mM KH_2PO_2, and 34 mM dextrose (pH 7.35). In *C. elegans* DA neurons, whole-cell currents were recorded by using electrodes pulled to 12–14 MΩ resistance and internal solution consisting of 125 mM K gluconate, 18 mM KCl, 4 mM NaCl, 0.6 mM $CaCl_2$, 1 mM $MgCl_2$, 10 mM Hepes, and 10 mM EGTA (pH 7.2 and 325 osmolarity), adjusted with sucrose. External solution contained 145 mM NaCl or $NMDG^+$, 5 mM KCl, 1 mM $CaCl_2$, 5 mM $MgCl_2$, 10 mM Hepes, and 20 mM D-glucose (pH 7.2 and 350 osmolarity). Data for single-channel analyses, acquired using FETCHAN and PSTAT software (Axon Instruments), were imported in ORIGIN 7.0 to construct channel-amplitude and open-time histograms. To facilitate the analysis, each recording was binned into 5,000-ms traces. Channel opening frequency was obtained by dividing the area used for the amplitude histograms by the time of the trace (5,000 ms). Traces that exhibited a number of channel events insufficient to perform the amplitude histograms were excluded (≈40–60% of all recordings). For noise analyses of WT DA neurons, two different DA concentrations were applied to the same cell, and a total of four DA concentrations were tested. Each trace was filtered with a 10-Hz high-pass filter. The mean currents and the variances measured in the absence of DA were subtracted from those measured when DA was present.

Uptake and Binding Assays. Three days after DAT-1 transfection, tsA-201 cells were washed twice with KRH buffer (120 mM NaCl or $MNDG^+$/4.7 mM KCl/1.2 mM KH_2PO_4/10 mM Hepes/2.2 $CaCl_2$/10 mM glucose/0.1 mM ascorbic acid, tropolone, and pargyline) and incubated with 50 nM [^{3}H]-DA (NEN) for 5 min at room temperature. For saturation analyses seven different concentrations of DA (0.001–2 μM) were applied. Uptake was terminated after three washes of ice-cold KRH buffer, and radioactivity was extracted by using 1% SDS for 20 min. Nonspecific uptake was determined by measuring [^{3}H]-DA accumulation in pcDNA3-transfected cells. We used the same protocol to measure [^{3}H]-DA accumulation in cultured *C. elegans* neurons. Three days after dissociation and plating, *C. elegans* embryonic cells were washed twice with external solution used for patch-clamp experiments. Uptake data were normalized to the number of DA neurons and counted by fluorescence-activated cell sorting by using a FACStar Plus flow cytometer (Becton Dickinson, San Jose, CA) equipped with a 488-nm argon laser and FITC filter set (Department of Veterans Affairs Medical Center/Vanderbilt University).

Binding of [^{3}H]-imipramine (IMP) (NEN) to intact tsA-201 cells expressing DAT-1 was performed for 1 h at 4°C. Three days after transfection, cells were washed twice with the same buffer used for uptake assay. Binding assays were initiated with the addition of 50 μl of [^{3}H]-IMP to each well containing 450 μl of buffer and terminated by four washes with ice-cold buffer. Specific binding was determined by the difference between total [^{3}H]-IMP binding and nonspecific binding measured in cells transfected with the empty vector. Binding and uptake data were normalized to the number of cells counted in parallel plates and analyzed by using PRISM4 (GraphPad, San Diego).

Results

Characterization of DAT-1 in Transfected Cells. To optimize the conditions for subsequent experiments in primary *C. elegans* neurons, and also to compare findings with our previous report of DAT activity in transfected HeLa cells (28), we measured uptake of radiolabeled DA ([^{3}H]-DA) in tsA-201 cells transiently transfected with *C. elegans* DAT (DAT-1). In DAT-1 expressing cells, [^{3}H]-DA accumulation increased in a concentration-dependent manner and saturated at ≈1 μM (Fig. 1*a*). These data fit well to a single-site Michaelis–Menten equation with V_{max} = 5.8 ± 0.3 attomole (amol)/min per cell and K_m = 170 ± 38 nM. IMP efficiently inhibited (IC_{50} = 49 ± 3 nM) DAT-1 activity (Fig. 1*b*) (28). Moreover, we found that [^{3}H]-DA uptake through DAT-1 is Na^+- and Cl^--dependent (Fig. 1*c*). Complete replacement of extracellular Na^+ ions by equimolar concentration of $NMDG^+$ decreased DA uptake by 98%, and substitution of gluconate for Cl ions decreased DA uptake by 70%. Uptake was essentially abolished in Na^+- and Cl^--free buffer (97% reduction).

Next, we sought to quantify the level of surface expression of DAT-1 in this model. To do so, we used ^{3}[H]-IMP binding as a measure of the number of DAT-1 transporters on the cell membrane. Because ^{3}[H]-IMP is a membrane-permeant compound, we determined the actual cell surface binding of ^{3}[H]-IMP by preincubating the cell with 1 mM DA for 10 min, and then we added five different concentrations (1–100 nM) of ^{3}[H]-IMP with DA still present in the buffer. DA preincubation blocks access of ^{3}[H]-IMP to surface DAT but will not affect ^{3}[H]-IMP binding to the intracellular DATs, because the assay is performed at 4°C, a temperature that does not support DA transport (28). Data from these studies fit a single-site binding equation (Hill coefficient = 0.7) with a B_{max} of 0.3 ± 0.03 amol per cell and a K_d of 25 ± 7 nM (Fig. 1*d*). We used this estimate to calculate the turnover rate for DA transport by DAT-1. The V_{max}/B_{max} ratio is 0.3. Assuming that each IMP binding site represents a single functional DAT-1 molecule, these findings

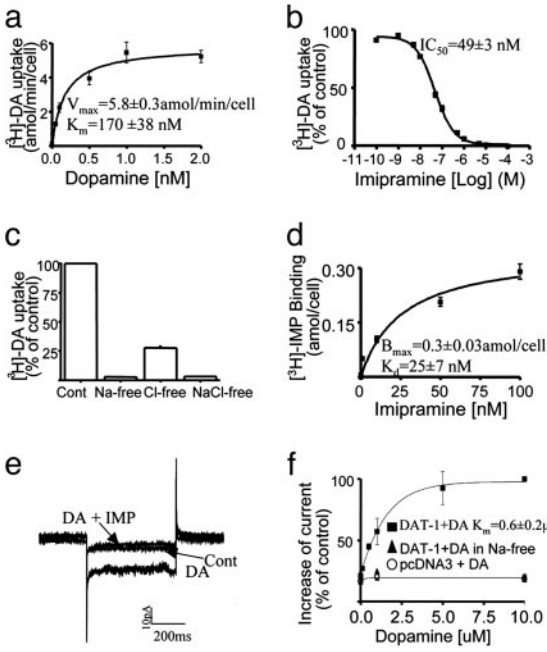

Fig. 1. Functional and electrophysiological characterization of DAT-1 in transiently transfected tsA-201 cells. (*a*) saturation kinetics of DA transport induced by DAT-1. (*b*) Inhibition of [^{3}H]-DA transport induced by DAT-1 by IMP. (*c*) Ion dependence of [^{3}H]-DA uptake measured in Na^+-, Cl^--, or NaCl-free buffer. (*d*) Saturation binding of [^{3}H]-IMP to DAT-1-transfected cells. [^{3}H]-DA was used at 50 nM in *a* and *c*; in *a*, DA concentrations higher than 50 nM were achieved by altering [^{3}H]-DA specific activity with unlabeled DA. Data are derived from at least three independent experiments. Individual data points were obtained in quadruplicate. (*e*) Representative traces of whole-cell patch-clamp currents. (*f*) Concentration dependence of DA-mediated currents measured at −120 mV (six to nine cells per point). The steady-state currents recorded at each concentration were normalized to the current recorded in DAT-1-transfected cells perfused with 10 μM DA. DA-induced (10 μM) inward currents (−22 ± 13 pA at −120 mV) were not detected when Na^+ ions were replaced by $NMDG^+$ (▲) or when the cells were transfected with pcDNA3 empty vector (○).

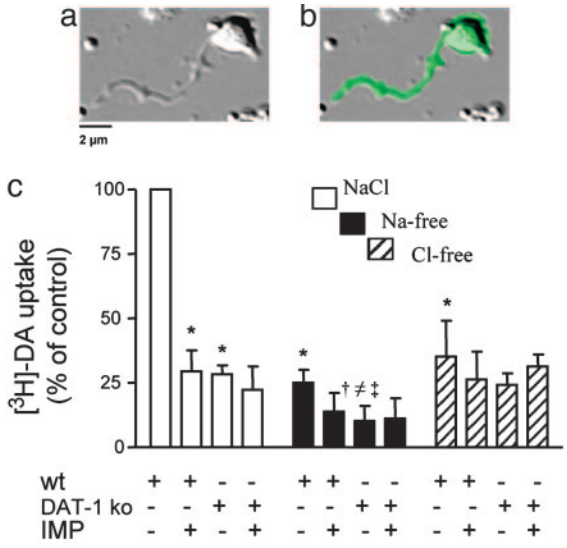

Fig. 2. DA transport in *C. elegans* neurons. (*a*) Differential interference contrast image of a typical $P_{dat\text{-}1}$::GFP (WT) *C. elegans* DA neuron shown as a GFP image in *b*. (*c*) Ionic dependence and inhibitor sensitivity of DA transport in *C. elegans* neurons. * and † indicate significant differences vs. WT in NaCl and Na^+-free buffer, respectively. ≠ and ‡ indicate significant differences vs. DAT-1 ko in NaCl and Cl^--free buffer, respectively. Means were compared by using one-way ANOVA and with $P \leq 0.01$.

indicate that, on average, one DA molecule is transported by DAT-1 every 3 seconds.

To test the electrogenicity of *C. elegans* DAT, we performed patch-clamp experiments in tsA-201 cells expressing DAT-1. Bath DA perfusion (2 μM) generated significant transport-associated inward currents and fluctuations (Fig. 1*e*) when the holding potential was stepped from −40 to −100 mV. These currents were inhibited by coperfusion with 10 μM IMP ($n = 6$). DA-induced current amplitude was fit to a single-site Michaelis–Menten equation with a K_m of 0.6 ± 0.2 μM (Fig. 1*f*). This value is higher than the K_m measured for uptake (0.17 μM) and may reflect the separate modes of carrier function and current generation in this transporter. Importantly, Na^+ replacement with $NMDG^+$ ions in the bath solution prevented DA-induced inward currents, and no DA-induced current was recorded in pcDNA3 vector-transfected cells (Fig. 1*f*). These results established the electrogenic nature of *C. elegans* DAT in transfected cells.

***C. elegans* DAT Accumulates DA in Native Cells.** We cultured DA neurons (Fig. 2 *a* and *b*) from *C. elegans* embryos as previously described (27). When we dissociated embryonic cells from $P_{dat\text{-}1}$::GFP, transgenic nematodes that express GFP in all DA neurons (24), the number of GFP-positive cells counted by fluorescence-activated cell sorting was found to be proportional to that expected in the mature embryo (≈0.5% of the total number of cells). Because the $P_{dat\text{-}1}$::GFP worm line expresses WT DAT-1, we will refer to this line as WT.

Even though the number of DA neurons (≈5,000) is a small fraction of the total number of cells cultured per well (10^6), we measured specific and significant accumulation of 50 nM [^{3}H]-DA (Fig. 2*c*). Such accumulation was reduced by 70% when measured in presence of 100 nM IMP, similar to the level of inhibition reached in transfected cells. To investigate whether the background 30% uptake represented residual DAT-1 activity insensitive to 100 nM IMP, we measured [^{3}H]-DA uptake in cultures prepared from *dat-1* ko animals ($P_{dat\text{-}1}$::GFP,*dat-1*(*ok157*) (*dat-1* ko) and obtained comparable results (Fig. 2*c*). Importantly, 100 nM IMP did not further inhibit [^{3}H]-DA uptake in *dat-1* ko cells. This finding strongly suggests that the residual uptake is not through DAT-1 but represents either binding or nonspecific uptake through uncharacterized transport systems. Saturation curves produced from six different concentrations (1–100 nM) of [^{3}H]-DA fit well to a single-site Michaelis–Menten equation with a V_{max} of 5.0 ± 0.2 amol/min per cell and a K_m of 35 ± 3.1 nM (data not shown).

tsA-201-transfected cells and native neurons show comparable V_{max} values; however, neurons have a 5-fold greater K_m than transfected cells. This finding likely reflects regulatory elements in neurons that are absent in the heterologous expression system. The Na^+ and Cl^- dependence of DAT-1 is, on the other hand, the same in neurons and transfected cells. [^{3}H]-DA uptake was decreased by 70% in WT neurons when extracellular Na ions were replaced by equimolar $NMDG^+$ (Fig. 2*c*). We observed no further significant inhibition of [^{3}H]-DA uptake by applying 100 nM IMP in Na^+-free buffer. We evaluated Cl^- dependence by replacing Cl^- with an equimolar concentration of gluconate and found that, in WT cells, [^{3}H]-DA uptake was reduced by 60% (Fig. 2*c*). IMP did not further reduce uptake in the absence of Cl^- in WT cells. Nonspecific [^{3}H]-DA uptake measured in *dat-1* ko cells was decreased by 65% in absence of Na^+, and 100 nM IMP did not further reduce residual transport (Fig. 2*c*). Because the *dat-1* ko does not express DATs, this result supports the idea that DA can be transported through another Na^+-dependent

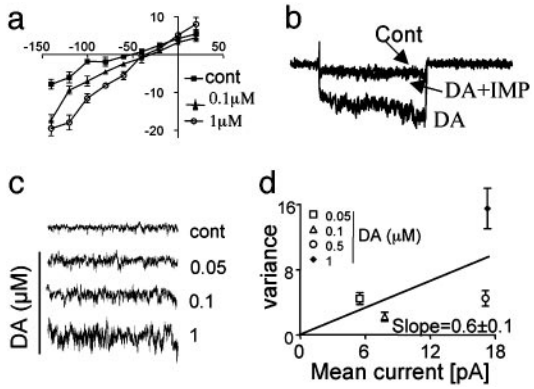

Fig. 3. Whole-cell recordings in *C. elegans* neurons. (*a*) A representative recording of the current–voltage relationship elicited in the absence (■) and presence of 0.1 (▲) and 1 (○) μM DA. (*b*) DA-mediated inward currents, recorded when the membrane potential was held at −40 and stepped to −100 mV, were blocked by IMP. (*c*) Extracellular DA application increased whole-cell current noise when the holding potential was held at −40 and stepped to −120 mV ($n = 7$). (*d*) Channel amplitude calculated as the slope of the linear regression curve obtained by plotting the mean currents and the variances measured when 0.05–1 μM DA were sequentially applied. Data are averages of six independent patches.

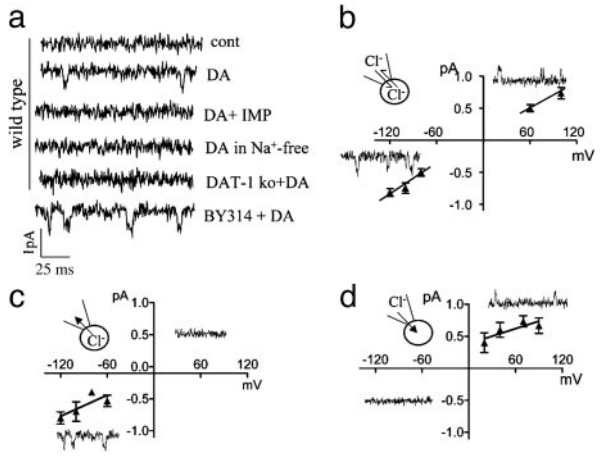

Fig. 4. Transporter channels in *C. elegans* DA neurons. (*a*) Channel events from WT and BY314 *C. elegans* DA neurons in outside-out patches at −120 mV. (*b–d*) Single-channel amplitude recorded in cell-attached configuration and plotted vs. the voltage, when the extracellular Cl^- concentration on both sides of the patch was equal to (*b*) or was lower (*c*) or higher (*d*) than the intracellular Cl^-.

transport system. In *dat-1* ko cells, DA accumulation also remained unaffected by gluconate replacement. These data confirm that DA uptake in *C. elegans* DA neurons is mediated primarily by DAT-1.

***C. elegans* DAT Is Electrogenic: Whole-Cell Recording in DA Neurons.** Whole-cell voltage-clamp experiments were performed in WT and *dat-1* ko DA neurons after 3–5 days in culture. Increasing concentrations of DA, sequentially applied to the bath solution, induced inward currents (Fig. 3*a*) when the membrane potential was ramped between −140 and 20 mV ($n = 6$). DA-induced inward currents were proportional to the concentration of DA applied and showed a more positive reversal potential (−35 ± 4 mV; $n = 6$) compared with that recorded in absence of DA (−50 ± 10 mV; $n = 6$; *t* test, $P < 0.05$). In current clamp, the membrane resting potential changed from −46 ± 5 mV to −38 ± 3 mV ($n = 6$; *t* test, $P < 0.05$) in the absence and in the presence of DA, respectively (data not shown). Reversal potentials determined from voltage clamp or current clamp were not statistically different (*t* test $P = 0.9$). Coperfusion of IMP (10 μM) with 1 μM DA consistently inhibited DA-induced inward current ($n = 5$; see Fig. 3*b*). We also detected no DA-induced current in whole-cell recordings from *dat-1* ko DA neurons ($n = 5$; data not shown). DA-induced inward currents recorded in the *C. elegans* DA neurons do not exhibit measurable transient currents (Fig. 3*b*), possibly because of the small density of DAT-1 in the cell body or the small size of the cells.

As in DAT-1-transfected cells, DA neurons demonstrated an increase in whole-cell current noise with DA application when the potential was stepped from −40 to −100 mV (Fig. 3*b*). Thus, we performed noise analysis of the stationary currents recorded from DA neurons in the absence and presence of different concentrations of DA (Fig. 3*c*). The variance (σ^2) measured at −120 mV in presence of 1 μM DA ($\sigma^2 = 15.5 \pm 3$ pA^2) was 10 times higher than in absence of DA ($\sigma^2 = 1.77 \pm 0.6$ pA^2; $n = 7$). By plotting σ^2 against the mean current for various DA concentrations, we calculated an average single-channel amplitude of $i = 0.6 \pm 0.1$ pA at −120 mV (Fig. 3*e*). These data encouraged us to look directly for single-channel activity in patches.

***C. elegans* DAT-1 Generates Single-Channel Currents: Patch-Clamp Analysis in Cultured DA Neurons.** To measure single-channel activity we used small, sharp pipettes (20 MΩ) to pull patches from *C. elegans* DA neurons. In the absence of DA we recorded occasional large (more than −3-pA) and brief (≈1-ms) channel events when the membrane potential was held at −120 mV. These spontaneous events were not blocked by IMP application, Na^+ removal, or *dat-1* genetic ablation (data not shown). Thus, they are unrelated to DAT-1. In presence of 1 μM DA, small (−0.8 ± 0.1 pA) single-channel events were recorded ($n = 7$) at −120 mV (Fig. 4*a*). These channels were abolished when 10 μM IMP was perfused with 1 μM DA ($n = 6$) or when external Na^+ was replaced by $NMDG^+$ ($n = 6$). DA-induced, single-channel events were absent in patches pulled from *dat-1* ko DA neurons ($n = 8$; see Fig. 4*a*). The concentration of DA we used could activate DA autoreceptors, and recent studies have identified DA receptors in *C. elegans* (31); however, these receptors are not expressed prominently in DA neurons. Nonetheless, to exclude the possibility that transporter channels result from DA receptor activation, all experiments were performed in presence of 1 μM butaclamol and spiperone (31), two DA receptor antagonists. Inhibitors that block DA receptors did not eliminate DA-induced channel events, whereas IMP blocked these currents. A recent report shows IMP to be an inhibitor of the EGL-2 (eag) K^+ channel (32). However, the concentration of IMP used in our study would be insufficient to inhibit the EGL-2 K^+ channel. Furthermore, DAT-mediated macroscopic and microscopic currents have a specific requirement for Na^+ and Cl^-, a characteristic of the SLC6A family to which DAT-1 belongs.

Ingram *et al.* (10) have shown that the DA-activated conductance in neurons is mainly because of Cl ions. To test whether Cl^- moves through the transporter channels that we observe, we performed single-channel recordings under various Cl^- conditions. When the electrode contained our intracellular solution (25 mM Cl^-), DAT channels appeared to reverse near 0 mV ($n = 7$; see Fig. 4*b*). When the electrodes contained low-Cl^- solutions (1 mM) and intercellular Cl^- was unaltered, DAT channels conducted only inward currents (Cl^- moved out; $n = 7$; see Fig. 4*c*). Moreover, after 2–4 h of incubation in low-Cl^- solutions, a condition that depletes intracellular Cl^- (16), transporter channels conducted only outward currents (Cl^- moved in; $n = 6$; see Fig. 4*d*). Although it was impossible to measure accurately, Fig.

NEUROSCIENCE

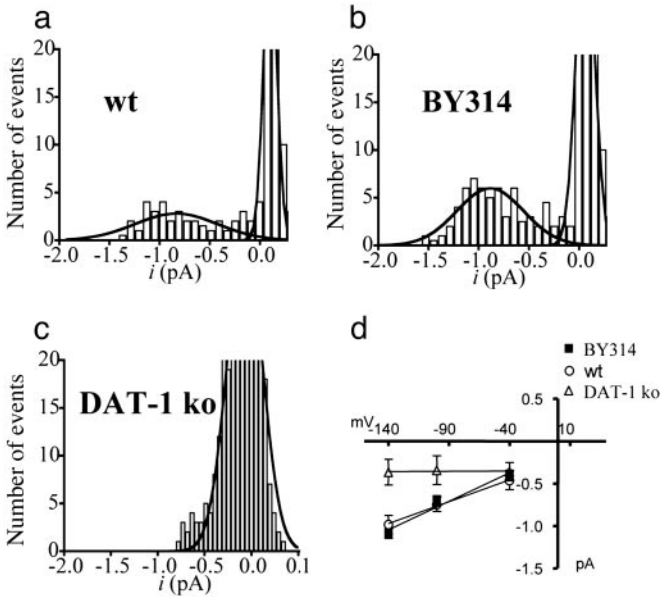

Fig. 5. Single-channel analyses of DAT-1 currents recorded at −120 mV. (*a–c*) Representative amplitude histograms from an outside-out patch containing DA-induced single-channel events in WT (*a*), BY314 (*b*), and *dat-1* ko (*c*) cells. Single-channel event amplitude measure in *a* and *b* was −0.8 ± 0.1 and 0.9 ± 0.06 pA, respectively. (*d*) Plot of single-channel amplitude vs. membrane potential in the presence of 1 μM DA of WT (○), BY314 (■), and *dat-1* ko (△) DA neurons. In *dat-1* ko neurons we recorded only background currents (±0.3 pA). Each symbol represents the mean ± SEM.

4 *c* and *d* also suggests a shift in reversal potential compatible with Cl^- permeability. From these experiments, we conclude that Cl^- ions permeate DAT-mediated single-channel currents.

Approximately 40% of membrane patches pulled from WT DA neurons exhibited single-channel activity. The remaining patches either had no channels or did not last long enough in the outside-out configuration to analyze the few events that did occur. To increase the probability of finding DA-sensitive channel events in patches, we created a transgenic line (BY314) that expresses, in addition to endogenous DAT-1, an NH_2-terminal GFP-tagged DAT-1 (GFP:DAT-1) in all *C. elegans* DA neurons, as demonstrated by GFP fluorescence in the whole animal image (data not shown). Cultured neurons from this line accumulated 30% more [^{3}H]-DA than WT (V_{max} = 7.8 ± 0.7 and 5 ± 0.2 amol/min per cell, respectively), with no difference in the K_m (37 ± 8 vs. 35 ± 3.1 nM, respectively). As expected, the number of patches exhibiting DAT-mediated channel events increased from 40% to 60%. Furthermore, frequency (*F*) and open probability were higher in BY314 neurons (F = 0.8 ± 0.04 Hz, and P = 0.006; n = 11) than in WT neurons (F = 0.5 ± 0.1 Hz, and P = 0.002; n = 8) (see Fig. 5 *a* and *b*). In contrast, the unitary conductance in the two worm lines (Fig. 5*d*) was not statistically different (5.2 ± 1.3 and 6.1 ± 0.8 pS in WT and BY314, respectively). DA-induced channels in BY314 DA neurons were Na^+- and IMP-sensitive (data not shown). Open-time histograms revealed that 72% of the transporter channels in BY314 neurons had nearly the same open time as WT neurons (6.9 ± 3 and 5.3 ± 3 ms, respectively). A subpopulation of BY314 channels (28%) exhibited longer open times (19.8 ± 3 ms).

Because IMP-sensitive channels were detected only in DA-treated WT and BY314 DA neurons, and because the probability of finding channel activity was higher in the BY314 neurons, which express the GFP DAT-1 translational fusion, whereas no DA-induced channels were recorded in *dat-1* ko neurons, we conclude that the IMP-sensitive channel events are associated exclusively with *C. elegans* DAT-1.

Discussion

Monoamine transporters, as well as GABA and glutamate transporters, have channel-like currents (18, 19, 21, 33, 34). In transfected cells, individual transporter channels have been observed; however, in native cells, these events have been inferred only from noise analysis (22). To date, no individual transporter-associated channels have been recorded in native cells, leaving open the question of whether transporter channels in actual neurons are large enough to play a significant physiological role. Previous work has shown that DAT-associated currents carried by Cl ions have a physiological role and increase neuron excitability (10). Such currents may be caused by the electrogenic properties of classical fixed-stoichiometry transporters, and it is unclear whether transporter channels play any part. Here we establish that single-channel events arising from DAT-1 in normally functioning DA neurons give rise to currents capable of depolarizing DA neurons. These channel currents appear to be carried by Cl ions and provide evidence for an underlying event supporting DAT-dependent Cl^- flux in neurons.

Twenty-four hours after cell isolation and plating, *C. elegans* DAT-1 cells send out neuron-like processes, which may synapse with other cells. Cultured DA neurons efficiently accumulate radiolabeled DA. Functional characterization of DAT in *C. elegans* embryonic neurons recapitulates the pharmacological and electrogenic properties seen in transfected cells, although DAT expressed in neurons is four times more efficient (V_{max}/K_m) than DAT-1 expressed in mammalian cells. DA accumulation and DA-induced currents are Na^+- and Cl^--dependent and IMP-sensitive. Moreover, no IMP-sensitive accumulation or DA-induced current occurs in neurons from *dat-1* ko animals. Finally, in neurons isolated from BY314 animals, where WT DAT is augmented with transgenic GFP-DAT, DA accumulation is higher than the WT cultures.

Leakage currents in the absence of substrates occur in DATs, serotonins, and norepinephrines in expression systems (9, 12, 13). We found no evidence of DAT-1-associated leak conductance in either DAT-1-transfected cells or native cells. Leak currents may be an artifact of heterologous expression, as shown for rat DAT (10).

Monoamine transporters have large substrate-induced currents, both in reconstituted systems and in native cells (9–13, 35), but the origin and the significance of these currents remain unclear. We calculated the current expected from classical transport by converting the DA transported (V_{max}) into current (pA) using Faraday's constant (96,000 C/mol). Comparing the amount of charges measured in the whole-cell current at resting potential (−46 mV) with the number of molecules expected from the observed transport (V_{max} = 5 ± 0.2 amol/min per cell), we calculated an excess of ≈100 charges moving through a single DAT per DA molecule transported. We may have underestimated the amount of DA transported due to metabolism or efflux; however, we obtained the same 100× factor in DAT-1-transfected cells. Whole-cell recordings in both transfected cells and *C. elegans* DA neurons show increased noise when DA is present. Fluctuation analysis implied channel events with amplitude (0.6 ± 0.1 pA at −120 mV), comparable to the channel amplitude (−0.8 ± 0.1 pA at −120 mV) recorded in patches. The overexpression of the GFP NH_2 terminus DAT-1 translational fusion did not alter the amplitude, but, as expected, if transporter channels were associated with normal DAT-1 function, both DA accumulation and channel frequency increased. Considering the frequency of single-channel events as the number of the events divided by the recording time, we calculated one channel event every 1.2 seconds in BY314 as compared with one event per 2

seconds in WT neurons. These numbers may overestimate DAT-1 channel frequency because we did not include patches with insufficient activity to perform the analysis.

We were unable to measure directly the number of transporters per cell in *C. elegans* neurons, possibly because of low surface density and high background binding with [^{3}H]-IMP or [^{125}I]-RTI55. However, we estimated N_{neuron} (the number of DATs in a single neuron) by assuming that the whole-cell current is proportional to the number of active transporters and using the equation

$$I_{cell}/N_{cell} = I_{neuron}/N_{neuron}, \quad [1]$$

where I_{cell} is the whole-cell current at rest, and N_{cell} represents B_{max} in DAT-1-transfected cells. I_{neuron} is the whole-cell current at rest in *C. elegans* DA neurons. We calculated N_{neuron} as 0.12 amol per cell (72,000 per cell). Using this number in the V_{max}/B_{max} ratio in *C. elegans* DA neurons, we estimated that one DA molecule moves through DAT every 1.5 seconds, which is close to the rate calculated for transfected cells (1 DA every 3seconds).

Both noise analyses and patch-clamp experiments reveal DAT-1-associated channels at −120 mV. We calculate N using the channel equation:

$$I = Nip, \quad [2]$$

where I stands for the whole-cell current, i is the single-channel current through an open transporter channel, and p is the probability of the channel being open. N is the total number of the transporter channels open or closed, and by this method N = 10,000 per cell. For p values, we assumed that a patch contained one channel (no additive i). The possibility exists for multiple channels at lower p, which would increase our estimate of N. Although patch area is uncertain and transporters are unevenly distributed, one might expect 10–100 channels per patch; however, forming a patch destroys activity, making it impossible to deduce channel density from patch data or vice versa (36). Interestingly, the number of the transporters measured by Eq. **1** is seven times higher than from Eq. **2**, suggesting that not all of the transporters on the cell surface are electrically active or behave as channels. We further note that, because of electrical inaccessibility, the whole-cell current is likely generated by transporters in the cell body rather than axon-dendrite processes, where DAT may concentrate (37). Thus, our estimate of 10,000 transporter channels per neuron may be an underestimate. Notwithstanding these uncertainties, it follows that the observed whole-cell currents, which depolarize *C. elegans* neurons, derive from transporter channels and not from electrogenic transport.

We further determined that Cl ions flux through transporter channels. With sufficient Cl^- on both sides of the channel, Cl ions move in either direction; when we skewed the Cl^- gradient in one direction or the other and varied no other ion, the observed currents and apparent reversal potential shift conformed to Cl^- flux. However, more experiments are required to quantify the degree of Cl^- selectivity or whether DA also moves through the transporter channel.

The transporter channels that account for macroscopic currents and depolarization in *C. elegans* DA neurons may also underlie the depolarizing currents in mammalian cells (10). Perhaps only a subpopulation of DATs exhibits a channel state when activated by DA, while most transporters behave classically, and these states may interconvert. Recent reports show that syntaxin interacts with the NH_2 terminus of norepinephrine (38) and serotonin (39) to inhibit substrate-induced currents. We speculate that *C. elegans* syntaxin (UNC-64) may bind DAT-1 as well and that increased channel events in BY314 neurons could arise from inhibition of this interaction because of GFP at the DAT-1 NH_2 terminus. The use of worm lines with alleles of unc-64 could test this hypothesis against single-channel activity. Regardless of these speculations and interpretations, we may conclude here that authentic channel states triggered by DA in a DAT reveal a novel mechanism to influence DA neuron excitability.

We acknowledge the efforts of Richard Nass in the generation and characterization of the BY200 line, Tammy Jessen for assistance with *C. elegans* husbandry, and Laura Bianchi for guidance in *C. elegans* electrophysiology. We thank Kevin Strange for critically reading the manuscript and for helpful discussion on *C. elegans* electrophysiology and cell cultures. Work was supported by National Institutes of Health (NIH)/National Institute on Drug Abuse Grant DA16338, NIH/National Institute of Neurological Disorders and Stroke Grant NS34075, and NIH/National Institute of Diabetes and Digestive and Kidney Diseases Grant PO1-DK 58212.

1. Uhl, G. R., Javitch, J. A. & Snyder, S. H. (1985) *Lancet* **1,** 956–957.
2. Kilty, J. E., Lorang, D. & Amara, S. G. (1991) *Science* **254,** 578–579.
3. Lorang, D., Amara, S. G. & Simerly, R. B. (1994) *J. Neurosci.* **14,** 4903–4914.
4. Ciliax, B. J., Heilman, C., Demchyshyn, L. L., Pristupa, Z. B., Ince, E., Hersch, S. M., Niznik, H. B. & Levey, A. I. (1995) *J. Neurosci.* **15,** 1714–1723.
5. Sesack, S. R., Hawrylak, V. A., Matus, C., Guido, M. A. & Levey, A. I. (1998) *J. Neurosci.* **18,** 2697–2708.
6. Krueger, B. K. (1990) *J. Neurochem.* **55,** 260–267.
7. McElvain, J. S. & Schenk, J. O. (1992) *Biochem. Pharmacol.* **43,** 2189–2199.
8. Gu, H., Wall, S. C. & Rudnick, G. (1994) *J. Biol. Chem.* **269,** 7124–7130.
9. Sonders, M. S., Zhu, S. J., Zahniser, N. R., Kavanaugh, M. P. & Amara, S. G. (1997) *J. Neurosci.* **17,** 960–974.
10. Ingram, S. L., Prasad, B. M. & Amara, S. G. (2002) *Nat. Neurosci.* **5,** 971–978.
11. Bruns, D., Engert, F. & Lux, H. D. (1993) *Neuron* **10,** 559–572.
12. Mager, S., Min, C., Henry, D. J., Chavkin, C., Hoffman, B. J., Davidson, N. & Lester, H. A. (1994) *Neuron* **12,** 845–859.
13. Galli, A., DeFelice, L. J., Duke, B. J., Moore, K. R. & Blakely, R. D. (1995) *J. Exp. Biol.* **198,** 2197–2212.
14. Jayanthi, L. D., Vargas, G. & DeFelice, L. J. (2002) *Br. J. Pharmacol.* **135,** 1927–1934.
15. Cammack, J. N., Rakhilin, S. V. & Schwartz, E. A. (1994) *Neuron* **13,** 949–960.
16. Wadiche, J. I., Amara, S. G. & Kavanaugh, M. P. (1995) *Neuron* **15,** 721–728.
17. Lester, H. A., Cao, Y. & Mager, S. (1996) *Neuron* **17,** 807–810.
18. Cammack, J. N. & Schwartz, E. A. (1996) *Proc. Natl. Acad. Sci. USA* **93,** 723–727.
19. Lin, F., Lester, H. A. & Mager, S. (1996) *Biophys. J.* **71,** 3126–3135.
20. DeFelice, L. J. & Blakely, R. D. (1996) *Biophys. J.* **70,** 579–580.
21. Galli, A., Blakely, R. D. & DeFelice, L. J. (1998) *Proc. Natl. Acad. Sci. USA* **95,** 13260–13265.
22. Larsson, H. P., Picaud, S. A., Werblin, F. S. & Lecar, H. (1996) *Biophys. J.* **70,** 733–742.
23. Sulston, J., Dew, M. & Brenner, S. (1975) *J. Comp. Neurol.* **163,** 215–226.
24. Nass, R., Hall, D. H., Miller, D. M., III, & Blakely, R. D. (2002) *Proc. Natl. Acad. Sci. USA* **99,** 3264–3269.
25. Nass, R. & Blakely, R. D. (2003) *Annu. Rev. Pharmacol. Toxicol.* **43,** 521–544.
26. Wintle, R. F. & Van Tol, H. H. (2001) *Parkinsonism Relat. Disord.* **7,** 177–183.
27. Christensen, M., Estevez, A., Yin, X., Fox, R., Morrison, R., McDonnell, M., Gleason, C., Miller, D. M., III, & Strange, K. (2002) *Neuron* **33,** 503–514.
28. Jayanthi, L. D., Apparsundaram, S., Malone, M. D., Ward, E., Miller, D. M., Eppler, M. & Blakely, R. D. (1998) *Mol. Pharmacol.* **54,** 601–609.
29. Brenner, S. (1974) *Genetics* **77,** 71–94.
30. Clark, S. G. & Chiu, C. (2003) *Development* **130,** 3781–3794.
31. Suo, S., Sasagawa, N. & Ishiura, S. (2003) *J. Neurochem.* **86,** 869–878.
32. Weinshenker, D., Wei, A., Salkoff, L. & Thomas, J. H. (1999) *J. Neurosci.* **19,** 9831–9840.
33. Galli, A., Blakely, R. D. & DeFelice, L. J. (1996) *Proc. Natl. Acad. Sci. USA* **93,** 8671–8676.
34. Wadiche, J. I. & Kavanaugh, M. P. (1998) *J. Neurosci.* **18,** 7650–7661.
35. Corey, J. L., Quick, M. W., Davidson, N., Lester, H. A. & Guastella, J. (1994) *Proc. Natl. Acad. Sci. USA* **91,** 1188–1192.
36. Ruknudin, A., Song, M. J. & Sachs, F. (1991) *J. Cell Biol.* **112,** 125–134.
37. Nirenberg, M. J., Chan, J., Vaughan, R. A., Uhl, G. R., Kuhar, M. J. & Pickel, V. M. (1997) *J. Neurosci.* **17,** 4037–4044.
38. Sung, U., Apparsundaram, S., Galli, A., Kahlig, K. M., Savchenko, V., Schroeter, S., Quick, M. W. & Blakely, R. D. (2003) *J. Neurosci.* **23,** 1697–1709.
39. Quick, M. W. (2003) *Neuron* **40,** 537–549.